Numerical Study on De-Icing of Aeroplane Wing Using Piezoelectric Materials

K. Guru Brahmam*, M. Chandra Sekhar Reddy, T Ramamohan Rao

* Department of Mechanical Engineering, Chaitanya Bharathi Institute of Technology, Gandipeta, Hyderabad, 500075, Telangana, India.
[2]Department of Mechanical Engineering, University College of Engineering (Autonomous), Osmania University, Hyderabad, 500007, Telangana, India.
[1]Department of Mechanical Engineering, Vasavi College of Engineering, Ibrahim Bagh, Hyderabad, 500089, Telangana, India.
Email: gurubrahmam_mech@cbit.ac.in

Abstract

The focus of the present investigation is to de-ice an airfoil wing using vibration induced by piezoelectric material. We selected symmetrical airfoil (NACA0015) for the numerical simulation. Airfoil is designed using solid works as airfoil data. Piezo electric patches and ice layer are designed and assembled to the airfoil wing using solid works. The final model is imported into ANSYS. Modal analysis is carried out for extraction of frequencies and mode shapes. Harmonic analysis is carried out for maximum shear stress. The results of these simulations allowed optimizing the positioning of the patches and angle of piezo on the structure and the optimal excitation voltage for the piezoelectric patches. Results are presented in the form of tabular data and digital photographs

Keywords: *De-Icing, wing, Piezoelectric Materials, Modal Analysis, Voltage.*

1. Introduction

Flight safety is undoubtedly the most important requirement for modern aircraft design and operation. However, in reality, aircraft flight performance and safety are inevitably affected by adverse meteorological conditions, one such weather condition is icing. Aircraft icing can cause severe aerodynamic and flight mechanical effects, thus threatens aircraft flight safety. Ice formation affects an airplane's performance by degrading its ability to generate lift. Ice accretes near the leading edge of an aircraft wing as it is a stagnation point. Ice deposition changes the leading-edge profile of the air foil and severely affects the lift generating ability of the wing. Ice formation takes place either on the ground or in flight.

The term de-icing means removal of the layer of ice from the surface of the body. Many de-icing techniques are implemented to prevent and remove ice from aircraft. The most commonly used de-icing techniques are chemical de-icing and anti-icing, electro-thermal de-icing, pneumatic de-icing, electro-impulse de-icing, and electro-vibratory de-icing. Piezoelectric de-icing, a new electro-vibratory de-icing technology, recently is proposed to apply to the aircrafts. This system has such characters as simple structure, less energy consumption and convenient maintenance. It is promising with low power requirement of the order of 1-3 kW which indicates good application prospect in the future.

2. Literature Review

The literature survey has revealed that several researchers attempted to find the widely interested study in a numerical model of a simple flat plate was elaborated to understand phenomena involved in vibration-based de-icing and assist with the design of the piezoelectric de-icing system. Ramanathan [1] et al. studied that resonating piezoelectric

*Corresponding author: E-mail: gurubrahmam_mech@cbit.ac.in

ISBN - 978-93-95038-50-8 https://doi.org/10.37285/bsp.sasat2023.08

elements were used to generate ultrasonic surface waves to produce shear stress at the ice interface and used an aluminum plate on which a piezoelectric actuator patch was bonded. The actuator was excited at a frequency of 1 MHz, the resonant frequency of the actuator, to remove an ice layer accreted a few centimeters ahead of the actuator. Delamination of the ice occurred after more than a hundred seconds and thermal energy released from the actuator played an important role in it. **Kandagal and Venkatraman [2]** investigated Similar to the de-icing mechanism explored by Venna partially, Kandagal and Venkatraman succeeded in de-icing a cantilevered flat plate with piezoelectric actuators by exciting its resonant frequencies. Excitation of the fourth mode, at 805 Hz, resulted in instantaneous delamination of the ice at several locations on the plate, without any trace of heating from the actuators. Analysis of the results showed that shear stress generated at the interface seemed to be responsible for breaking the ice adhesion to the substrate.**M. Matbou Riahi [3],** et al. mainly examines the mechanical behavior at the ice/aluminum interface in order to develop a numerical model simulating de-icing. The numerical results obtained using the beam theory show important differences compared to experimental data. **Tian Baz [4]** et al studied the analytic and experimental research of a vibration de-icing method for aircrafts with piezoelectric transducer as the actuator. The power consumption for vibration de-icing is about 36.5 w/m^2, which is only 1.57 % of the power consumption when using the latest electro-thermal de-icing method. **Palacios [5]** et al. studied ultrasonic waves and their dispersion on a flat plate. It was showed that as the excitation frequency approached the resonant frequency of the actuator, the adhesion of the ice diminished, and the plate temperature increased. The study concluded that the excitation frequency should be below 100 kHz since strains generated diminished with a frequency increase. **Kalkowski [6]** et al. used numerical simulations to estimate the shear stress at the interface generated by piezoelectric actuators and the matching power consumption of the actuators. **Habibi [7]** et al. investigated the use of piezoelectric actuators to excite shear stresses on Carbon-Fiber-Reinforced Polymer (CFRP) as a de-icing system. They used FEM to study the wave propagation through this material. With the results they established an optimal excitation of the system by comparing the resulting shear stress with the adhesive shear strength of ice. The obtained results will be tested experimentally in a later study. **Budinger [8]** et al. developed an analytical model for piezoelectric de-icing at ultrasonic frequencies. The model showed that flexural modes generate more shear stress at the ice/substrate interface than extensional modes.

Yin [9] et al. studied a new non-thermal method–ultrasonic de-icing for wind turbine blade is proposed. Firstly, based on the theory of ultrasonic de-icing, the harmonic analysis of the structure of the composite plate-ice layered system is investigated using the finite element method. The simulation results showed that ultrasonic de-icing method is feasible for wind turbine blade de-icing purposes. **Palacios [10]** implemented a 3D finite element model and used it to design de-icing system experimental setups. With the help of this tool, they investigated the impedance matching for excitation, which lead to promising experimental results. **Yihua Cao [11] et al,** a brief review of the research on aircraft icing is presented. The following aspects are discussed. First, the causes, types, severity and natural parameters of aircraft icing are introduced. Then, the various effects of ice accretion on aircraft aerodynamic performance, stability, controllability as well as the existing estimation methods are summarized and analyzed. **Prashanth Sagar Reddy, Beeram [12] et al. C**omprehensive study was conducted to characterize ice adhesion strength over various surfaces by using a custom-built shear strength tester. **Boutros [13]**proposed a de-icing solution using lightweight Macro Fiber Composite (MFC) actuators on the leading edge of a wing. The developed numerical model for MFC actuators was validated experimentally on cantilever beams. **Harvey [14]** followed by **Villeneuve [15] et al.** demonstrated a proof of concept for de-icing with actuator patches at structural resonant frequencies matching the first modes of the structures on which they were bonded. Total or partial de-icing was successfully achieved for a flat plate, a thinned Bell 206 main rotor blade, and a Bell 206 tail rotor blade sections. Numerical simulations were used to predict the resonant frequencies and the mode shapes to optimally position and drive the actuators.

In this paper The modal analysis of Testing Skin with Piezoelectric Ceramics is done by generating mesh and giving fixed support. The following frequencies and their corresponding mode shapes are extracted as the result of modal analysis. Harmonic Analysis is carried out for maximum shear stress by taking frequencies extracted from modal analysis and voltage as input, evaluating results, Observing and recording shear stress.

The Harmonic analysis is carried out with the frequency from 0 to 1000Hz and the excitation voltage 300V. The maximum shear stress is obtained with the natural frequency 977.5 Hz in harmonic response. The above procedure is repeated with PZT at different locations on the wing.

3. PROBLEM STATEMENT

The finite element analysis software ANSYS has been proved effective in years of applications on vibration analysis, it is employed here to investigate the influence of the length of piezoceramic actuator to the vibration excitation of the wing. In the finite element model the length of the wing is 395 mm and the thickness is 2mm, and the material properties are also defined. The material of the square actuator is PZT5H with the thickness 0.5mm. The wing is fixed on one side, and multiple PZT patches are bonded on the plate at the wave crest or trough where produces the largest strain energy. Alternating voltage is applied to the PZT to excite the vibration of the wing through reverse piezoelectric effect, and the length of the PZT will be changed to search for its relationship with the vibration intensity of certain mode. For our model we have taken 50.8x50.8x0.5mm as PZT dimensions as we are studying wing with smaller dimensions when compared to original aeroplane wing.

4. RESEARCH METHODOLOGY

This numerical model was developed to design and predict optimal excitation of structures for de-icing purpose. This study allowed to develop a numerical model of a wing with piezoelectric patches and understand optimal phasing of the actuators. The numerical model is used in the further phase of the project by adding ice layers for investigation of vibration-based de-icing, with the final objective of developing and integrating a piezoelectric actuator de-icing system to an Aircraft wing structure.

The results of these simulations allowed to optimize the positioning of the actuators on the structure and the optimal phasing of the actuators for mode activation. A numerical model of the final setup was elaborated with the piezoelectric actuators optimally positioned on the wing and meshed with piezoelectric elements. Electrical boundary conditions were applied to the actuators to excite the vibration of the Aero plane wing. The results validated the model when the Aero plane wing is optimally excited.

4.1. Flow Chart for Simulation

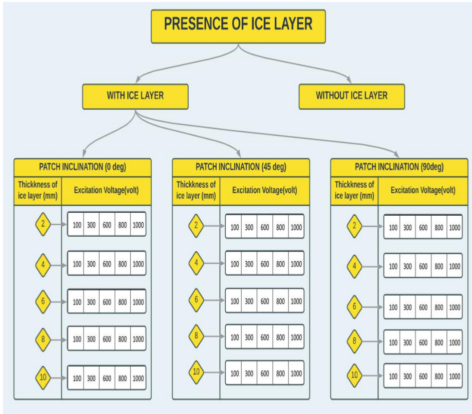

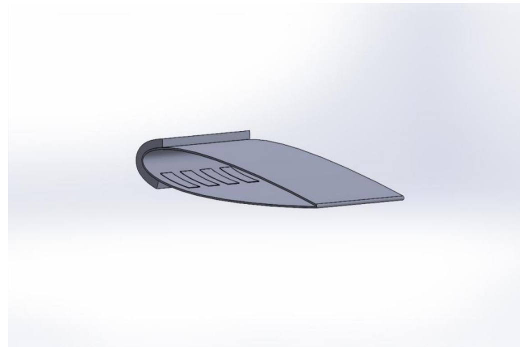

Figure 1. Flow chart for analysis
.

Figure 2. Design of aero plane wing with PZT patch and Ice Layer in Solid works

4.2. Design of aero plane wing with PZT patch and ice layer

After modelling of airfoil wing ice layer is assembled on the leading edge of the wing with different thickness for each model. Piezoelectric patches are also attached to the wing at different locations and in different numbers.

4.3 Modal analysis and harmonic response on aero plane wing with piezoelectric patches and ice layer

Table 1. Modal analysis

Tabular Data

	Mode	Frequency [Hz]
11	11.	575.33
12	12.	667.91
13	13.	692.4
14	14.	707.96
15	15.	710.62
16	16.	815.97
17	17.	828.07
18	18.	840.82
19	19.	913.81
20	20.	929.39

4.4 Summary

The de-icing of Aero plane wing using piezo electric material has been done using SOLID WORKS and ANSYS. The modal and harmonic analysis of aero plane wing has been done. Mode shapes and frequencies are obtained from modal analysis and from the harmonic analysis we can determine the shear stress required to break the ice. To remove ice successfully from aluminum wing we need 0.52 MPa of shear stress. To achieve this goal, trial and error voltages have been taken and resulting shear stress values are found and recorded. The results obtained from harmonic response are compared with the literature study. These results would further be interpreted in results and discussion.

5. Results and Discussion

The main objective of our work is to break ice on the Aero plane wing by applying voltage to the PZT and getting required shear stress at that particular location, so ice adhesion properties are also studied while doing project, the same details are mentioned below Ice adhesion is based on physical and chemical processes that exist between the ice and solid interface. In general, the adhesion forces can be categorized into three different types: chemical adhesion that includes covalent and electrostatic forces; thermodynamic adhesion involving van der Waals forces and hydrogen bonding; mechanical adhesion due to solid surface roughness. So, from reference paper (characterisation of ice adhesion strength over different surfaces pertinent to aircraft anti-/de-icing by Prasanth Sagar Reddy Beeram) we have taken ice adhesion strength of aluminium alloy taken as 0.09Mpa for aluminium 6061.

We have recorded shear stress values on the aero plane wing by giving different voltages to the PZT material in the ANSYS simulation software, and the same process is repeated for various models with PZT at different locations from the fixed end.

We have analysed harmonic response at maximum deformation frequency as mentioned in the methodology chapter. So, for the first model we obtained shear stress values for different voltage inputs and the same process is repeated for remaining models. The same is presented below as tabular form.

Table 2. Shear stress values of the first mode with 100V

S.NO	Frequency (Hz)	Max shear stress (MPa)	Shear stress (XY) MPa	Shear stress (YZ) MPa	Shear stress (XZ)MPa
1	150	0.0090787	0.0041753	0.0028347	0.0061255
2	200	0.0090233	0.0040877	0.0028384	0.0060105
3	250	0.0090367	0.0041114	0.0028364	0.0060394
4	300	0.0090515	0.0041214	0.0028368	0.0060419
5	350	0.0090523	0.004128	0.0028421	0.0061272
6	400	0.0090868	0.0041922	0.0028377	0.0061084
7	450	0.0090212	0.0040642	0.0028345	0.0060486
8	500	0.0090377	0.0040893	0.00283	0.0060705
9	550	0.0089735	0.0040647	0.0027886	0.0059402
10	600	0.0090941	0.0041259	0.0028569	0.006181

Table 3. Shear stress values for second mode with 100V

S.No	Frequency (Hz)	Max shear stress (MPa)	Shear stress (XY) MPa	Shear stress (YZ) MPa	Shear stress (XZ)MPa
1	150	0.047805	0.028671	0.023949	0.018797
2	200	0.047679	0.028438	0.023983	0.018737
3	250	0.047717	0.028472	0.023976	0.018757
4	300	0.047722	0.028499	0.023973	0.018793
5	350	0.047751	0.02852	0.023974	0.018789
6	400	0.047802	0.028645	0.02393	0.018886
7	450	0.047575	0.028333	0.024006	0.018724
8	500	0.047624	0.028216	0.023995	0.01877
9	550	0.047244	0.02769	0.024063	0.019022
10	600	0.047828	0.028724	0.023961	0.018759

Table 4. Shear stress values for third mode with 100V

S.No	Frequency (Hz)	Max shear stress (MPa)	Shear stress (XY) MPa	Shear stress (YZ) MPa	Shear stress (XZ)MPa
1	100	0.0041437	0.0017046	0.00089307	0.0017183
2	200	0.0041367	0.0017005	0.00089199	0.0017173
3	300	0.0042967	0.0017104	0.0010235	0.0015551
4	400	0.0041605	0.0017051	0.0008961	0.0016993
5	500	0.0041548	0.0017085	0.00088868	0.0017229
6	600	0.0041368	0.0017103	0.00089164	0.001763
7	700	0.0046788	0.0035704	0.0024507	0.0023381
8	800	0.016048	0.0077932	0.0079443	0.0054846
9	900	0.0042071	0.0016178	0.00095532	0.0016707
10	1000	0.0041521	0.0017054	0.00088702	0.0017061

Table 5. Shear Stress values for the fourth mode with 300V

S.NO	Frequency (Hz)	Max shear stress (MPa)	Shear stress (XY) MPa	Shear stress (YZ) MPa	Shear stress (XZ)MPa
1	122.5	0.076108	0.021041	0.061969	0.018795
2	145	0.075702	0.021277	0.06155	0.018959
3	302.5	0.076452	0.020846	0.06236	0.018698
4	415	**0.11178**	0.058249	0.069522	0.05213
5	527.5	0.076852	0.020822	0.062816	0.018579
6	572.5	0.076767	0.020731	0.062683	0.018713
7	617.5	0.076698	0.020818	0.062694	0.018938
8	662.5	0.076609	0.020773	0.062498	0.018495
9	707.5	0.076529	0.020773	0.062444	0.018623
10	752.5	0.076261	0.021019	0.062438	0.018739
11	797.5	0.076037	0.021127	0.06213	0.018907
12	842.5	**0.76507**	**0.60332**	**0.17558**	**0.12334**
13	887.5	0.077714	0.021307	0.063222	0.018623
14	977.5	**1.0086**	**0.84915**	**0.4491**	**0.35533**
15	1000	0.076801	0.021104	0.06257	0.018458

Table 6. Shear Stress values for the fifth mode with 300V

S.NO	Frequency (Hz)	Max shear stress (MPa)	Shear stress (XY) MPa	Shear stress (YZ) MPa	Shear stress (XZ)MPa
1	150	0.14342	0.086013	0.071847	0.056392
2	200	0.14304	0.085313	0.07195	0.056211
3	250	0.14315	0.085417	0.071927	0.056271
4	300	0.14317	0.085496	0.071918	0.056378
5	350	0.14325	0.085559	0.071922	0.056368
6	400	0.14341	0.085934	0.07179	0.056659
7	450	0.14273	0.084998	0.072018	0.056173
8	500	0.14287	0.084649	0.071985	0.05631
9	550	0.14173	0.083071	0.07219	0.057065
10	600	0.14348	0.086172	0.071883	0.056278

Table 7. Shear Stress values for sixth mode with 600V

S.NO	Frequency(Hz)	Max shear stress(MPa)	Shear stress(XY) MPa	Shear stress(YZ) MPa	Shear stress(XZ)MPa
1	190	0.31488	0.07216	0.1436	0.031461
2	280	0.31481	0.072054	0.14352	0.03156
3	370	0.31499	0.072247	0.14365	0.031368
4	460	0.31493	0.072198	0.14362	0.031438
5	540	0.31501	0.07214	0.14359	0.031497
6	640	0.31481	0.072155	0.14358	0.031529
7	730	0.3147	0.072095	0.14353	0.031661
8	820	0.31439	0.071368	0.14296	0.032954
9	910	0.31522	0.072447	0.14372	0.030746
10	1000	0.31501	0.072231	0.14362	0.031242

Table 8. Shear Stress values for seventh mode with 600V

S.NO	Frequency (Hz)	Max shear stress (MPa)	Shear stress (XY) MPa	Shear stress (YZ) MPa	Shear stress (XZ)MPa
1	150	0.054472	0.025052	0.017008	0.036753
2	200	0.05414	0.025052	0.01703	0.036063
3	250	0.05422	0.024669	0.017018	0.036236
4	300	0.054309	0.024728	0.017021	0.036252
5	350	0.054314	0.024768	0.017053	0.036763
6	400	0.054314	0.025153	0.017026	0.03665
7	450	0.054127	0.024536	0.017007	0.036291
8	500	0.054226	0.024536	0.01698	0.036423
9	550	0.053841	0.024388	0.016732	0.035641
10	600	0.054565	0.024755	0.017141	0.037086

Table 9. Shear Stress values for seventh mode with 600V

S.NO	Frequency (Hz)	Max shear stress (MPa)	Shear stress (XY) MPa	Shear stress (YZ) MPa	Shear stress (XZ) MPa
1	150	0.06387	0.011677	0.011677	0.036174
2	200	0.063744	0.015502	0.011697	0.03598
3	250	0.063774	0.015567	0.01168	0.036072
4	300	0.06387	0.015597	0.011698	0.036069
5	350	0.06385	0.01563	0.011667	0.03116
6	400	0.064031	0.015997	0.01653	0.036333
7	450	0.063706	0.015336	0.011693	0.036176
8	500	0.063657	0.015477	0.011681	0.03624
9	550	0.064247	0.015628	0.011786	0.037548
10	600	0.06392	0.015753	0.011628	0.036127

Table 10 Shear Stress values for ninth mode with 800

S.NO	Frequency (Hz)	Max shear stress (MPa)	Shear stress (XY) MPa	Shear stress (YZ) MPa	Shear stress (XZ)MPa
1	150	0.08516	0.021009	0.015569	0.048232
2	200	0.084993	0.020669	0.015596	0.047974
3	250	0.085032	0.020756	0.015574	0.048096
4	300	0.08516	0.02084	0.015597	0.048092
5	350	0.085133	0.02084	0.015569	0.048155
6	400	0.085374	0.02133	0.015537	0.048445
7	450	0.084941	0.020448	0.01559	0.048235
8	500	0.084876	0.020636	0.015574	0.04832
9	550	0.085663	0.020837	0.015715	0.050065
10	600	0.085227	0.021003	0.015504	0.048169

Table 11.: Shear Stress values for tenth mode with 800V

S.NO	Frequency (Hz)	Max shear stress (MPa)	Shear stress (XY) MPa	Shear stress (YZ) MPa	Shear stress (XZ)MPa
1	150	0.072629	0.033403	0.022678	0.049004
2	200	0.072186	0.032702	0.022707	0.048084
3	250	0.072294	0.032892	0.022691	0.048315
4	300	0.072412	0.032971	0.022694	0.048335
5	350	0.072412	0.033024	0.022737	0.049017
6	400	0.072694	0.033537	0.022701	0.048867
7	450	0.072169	0.032514	0.022676	0.048389
8	500	0.072301	0.032714	0.02264	0.048564
9	550	0.071788	0.032518	0.022309	0.047522
10	600	0.072753	0.033007	0.022855	0.049448

Table 12. Shear stress values for Eleventh model for the excitation voltage of 1000V

S.NO	Frequency (Hz)	Max shear stress (MPa)	Shear stress (XY) MPa	Shear stress (YZ) MPa	Shear stress (XZ)MPa
1	122.5	**0.76108**	0.21041	0.61969	0.18795
2	145	0.76108	0.21277	0.6155	0.18959
3	167.5	0.89829	0.4111	0.71335	0.17614
4	190	0.77024	0.20903	0.63032	0.18518
5	212.5	0.76737	0.20771	0.62689	0.18605
6	235	0.76624	0.20742	0.62558	0.1864
7	257.5	0.76555	0.20783	0.6248	0.18662
8	280	0.76511	0.20811	0.62415	0.18681
9	302.5	0.76452	0.20846	0.6236	0.18698
10	325	0.76393	0.20883	0.62294	0.18719
11	347.5	0.76312	0.20932	0.62208	0.18745
12	370	0.76197	0.21011	0.62074	0.1877
13	392.5	0.75926	0.21153	0.61782	0.18927
14	415	1.1178	0.58249	0.69522	0.5213
15	437.5	0.85768	0.33312	0.69147	0.16607
16	460	0.77639	0.21219	0.63619	0.18285
17	482.5	0.77147	0.20978	0.63114	0.18285

Contd…

S.NO	Frequency (Hz)	Max shear stress (MPa)	Shear stress (XY) MPa	Shear stress (YZ) MPa	Shear stress (XZ)MPa
18	505	0.76972	0.20866	0.62915	0.18533
19	527.5	0.76852	0.20822	0.62816	0.18579
20	550	0.7684	0.2087	0.62755	0.18614
21	572.5	0.76767	0.20731	0.62683	0.18713
22	595	0.76698	0.20729	0.62673	0.18732
23	617.5	0.76647	0.20818	0.62694	0.18938
24	640	0.76679	0.20974	0.62415	0.18743
25	662.5	0.76609	0.20773	0.62498	0.18495
26	685	0.76566	0.20757	0.62481	0.18575
27	707.5	0.76529	0.20789	0.62444	0.18623
28	730	0.76471	0.20789	0.62444	0.1868
29	752.5	0.76261	0.2082	0.62379	0.18739
30	775	0.76213	0.21019	0.62438	0.18758
31	797.5	0.76037	0.21019	0.62309	0.18907
32	820	0.75933	0.21127	0.6213	0.19562
33	842.5	7.6507	0.22121	0.61975	1.2334
34	865	0.76394	6.0332	0.61975	0.18458
35	887.5	0.77714	0.21948	1.7558	0.18623
36	910	0.7719	0.21307	0.62773	0.18623
37	932.5	0.77013	0.21019	0.63222	0.18667
38	955	0.77026	0.20888	0.63066	0.18912
39	977.5	**10.086**	8.4915	4.491	3.5533
40	1000	0.76801	0.21104	0.6257	0.18458

Table 13. Shear Stress values for twelfth mode with 1000V

S.NO	Frequency (Hz)	Max shear stress (MPa)	Shear stress (XY) MPa	Shear stress (YZ) MPa	Shear stress (XZ)MPa
1	122.5	**0.76108**	0.21041	0.61969	0.18795
2	145	0.76108	0.21277	0.6155	0.18959
3	167.5	0.89829	0.4111	0.71335	0.17614
4	190	0.77024	0.20903	0.63032	0.18518
5	212.5	0.76737	0.20771	0.62689	0.18605
6	235	0.76624	0.20742	0.62558	0.1864
7	257.5	0.76555	0.20783	0.6248	0.18662
8	280	0.76511	0.20811	0.62415	0.18681
9	302.5	0.76452	0.20846	0.6236	0.18698
10	325	0.76393	0.20883	0.62294	0.18719
11	347.5	0.76312	0.20932	0.62208	0.18745
12	370	0.76197	0.21011	0.62074	0.1877
13	392.5	0.75926	0.21153	0.61782	0.18927
14	415	1.1178	0.58249	0.69522	0.5213
15	437.5	0.85768	0.33312	0.69147	0.16607
16	460	0.77639	0.21219	0.63619	0.18285
17	482.5	0.77147	0.20978	0.63114	0.18285
18	505	0.76972	0.20866	0.62915	0.18533
19	527.5	0.76852	0.20822	0.62816	0.18579
20	550	0.7684	0.2087	0.62755	0.18614

Contd…

S.NO	Frequency (Hz)	Max shear stress (MPa)	Shear stress (XY) MPa	Shear stress (YZ) MPa	Shear stress (XZ)MPa
21	572.5	0.76767	0.20731	0.62683	0.18713
22	595	0.76698	0.20729	0.62673	0.18732
23	617.5	0.76647	0.20818	0.62694	0.18938
24	640	0.76679	0.20974	0.62415	0.18743
25	662.5	0.76609	0.20773	0.62498	0.18495
26	685	0.76566	0.20757	0.62481	0.18575
27	707.5	0.76529	0.20789	0.62444	0.18623
28	730	0.76471	0.20789	0.62444	0.1868
29	752.5	0.76261	0.2082	0.62379	0.18739
30	775	0.76213	0.21019	0.62438	0.18758
31	797.5	0.76037	0.21019	0.62309	0.18907
32	820	0.75933	0.21127	0.6213	0.19562
33	842.5	7.6507	0.22121	0.61975	1.2334
34	865	0.76394	6.0332	0.61975	0.18458
35	887.5	0.77714	0.21948	1.7558	0.18623
36	910	0.7719	0.21307	0.62773	0.18623
37	932.5	0.77013	0.21019	0.63222	0.18667
38	955	0.77026	0.20888	0.63066	0.18912
39	977.5	**10.086**	8.4915	4.491	3.5533
40	1000	0.76801	0.21104	0.6257	0.18458

The coupling element type is PZT for the piezoelectric material (Patch) and Aluminium for testing skin i.e., wing. The freedom of the nodes on the testing edge is constrained too. However, the deformation position of the testing skin with PZT patch differs a little from the skin without PZT patches. As we have already discussed in methodology, we have taken PZT patches at different locations and studied shear stress at different voltages for each location. The harmonic analysis is carried out with the frequency extracted from modal analysis and corresponding shear stress varying with different voltage inputs is illustrated in above figures.

As we have discussed the ice adhesion strength for aluminium alloy is 0.52 MPa. Once the shear stress at that location reaches ice adhesive shear strength, this force can remove the ice adhered to the skin, which means it is feasible to design this piezoelectric de-icing system in this Simulation of “De-icing on aero plane wing with piezo electric material”.

6. CONCLUSION

The existing de-icing methods have some disadvantages. To solve these problems, de-icing with piezo electric materials is studied in this project. Piezoelectric materials are used and bonded on the surface of the structure to act as the actuators. At different PZT locations, shear stress values are determined at maximum deformation frequency. To remove ice successfully from aluminum wing we need 0.52 MPa of shear stress. To achieve this goal, trial and error voltages have been taken and resulting shear stress values are found and recorded.

Based on the Numerical Analysis and Simulation in ANSYS, the following conclusions can be drawn: The present method can be used to remove ices at any position when the piezoelectric patches are evenly distributed on the whole structure. On the other hand, when the icing positions are fixed, through the reasonable arrangement of piezoelectric patches, less piezoelectric patches are needed.

REFERENCES

1. Ramanathan, S. An Investigation on the Deicing of Helicopter Blades Using Shear Horizontal Guided Waves. Ph.D. Thesis, The Pennsylvania State University, University Park, PA, USA, 2005.
2. Kandagal, S.; Venkatraman, K. Piezo-actuated vibratory deicing of a flat plate. In Proceedings of the 46th AIAA/ASME/ASCE/AHS/ASC Structures, Structural Dynamics and Materials Conference, Austin, TX, USA, 18–21 April 2005; p. 2115
3. M. Matbou Riahi, D. Marceau a, C. Laforte, J. Perron The experimental/numerical study to predict mechanical behaviour at the ice/aluminum interface (2011)
4. Tian Baz, Chunling Zhu, Bo Miao, Kai Li, Chengxiang Zhu., Vibration de-icing method with piezoelectric actuators (2014)
5. Palacios, J.L.; Zhu, Y.; Smith, E.; Rose, J. Ultrasonic Shear and Lamb Wave Interface Stress for Helicopter Rotor Deicing Purposes. In Proceedings of the 47th Structures, Structural Dynamics and Materials Conference, Newport, RI, USA, 1–4 May 2015.
6. Kalkowski, M.; Waters, T.; Rustighi, E. Removing surface accretions with piezo-excited high-frequency structural waves. In Active and Passive Smart Structures and Integrated Systems 2015; International Society for Optics and Photonics: Bellingham, WA, USA, 2015.
7. Habibi, H.; Chong, A.; Kanfoud, J.; Selcuk, C.; Gan, T.H.; Mayhew, D. Simulation of an electro-mechanical ice protection system for aircraft structure based on ultrasonic guided wave. In Proceedings of the Greener Aviation 2016, Brussels, Belgium, 11–13 October 2016.
8. Budinger, M.; Pommier-Budinger, V.; Napias, G.; Costa da Silva, A. Ultrasonic Ice Protection Systems: Analytical and Numerical Models for Architecture Tradeoff. J. Aircr. 2016, 53, 680–690.
9. Congbo Yin, Zhendong Zhang, Zhenjun Wang, Hui Guo. Numerical simulation and experimental validation of ultrasonic de-icing system for wind turbine blade (2016)
10. Palacios, J.; C Smith, E.; Zhu, Y.; L Rose, J.; Morrow, P. Global Ultrasonic Shear Wave Anti-Icing Actuator for Helicopter Blades. In Annual Forum Proceedings-American Helicopter Society; American Helicopter Society, Inc.: Virginia Beach, VA, USA, 2017.
11. Aircraft icing: an ongoing threat to aviation safety (2017) Yihua Cao, Wenyuan Tan, Zhenlong Wu.
12. by Prashanth Sagar Reddy Beeram Characterization of ice adhesion strength over different surfaces pertinent to aircraft anti-/de-icing (2017).
13. Boutros Azizi, Richard J. Prazenica, and Daewon Kim, Finite Element Modeling of Macro-Fiber Composite Actuators for Wing De-Icing Applications (2018).
14. LI Qingying, ZHU Yongjiu, Analysis of the Application of Piezoelectric Ceramic Material in the De-Icing Technique of the Aircrafts (2018).
15. Villeneuve, E.; Harvey, D.; Zimcik, D.; Aubert, R.; Perron, J. Piezoelectric De-Icing System for Rotorcraft. J. Am. Helicopter Soc. (2020).